9-13-2012

New half-lives of r-process Zn and Ga isotopes measured with electromagnetic separation

M. Madurga
The University of Tennessee, Knoxville

R. Surman
Union College, Schenectady

I. N. Borzov
Joint Institute for Nuclear Research, Dubna

R. Grzywacz
The University of Tennessee, Knoxville

K. P. Rykaczewski
ORNL Physics Division

See next page for additional authors

Recommended Citation

Madurga, M., Surman, R., Borzov, I., Grzywacz, R., Rykaczewski, K., Gross, C., Miller, D., Stracener, D., Batchelder, J., Brewer, N., Cartegni, L., Hamilton, J., Hwang, J., Liu, S., Ilyushkin, S., Jost, C., Karny, M., Korgul, A., Królas, W., Kuniak, A., Mazzocchi, C., Mendez, A., Miernik, K., Padgett, S., Paulauskas, S., Ramayya, A., Winger, J., Wolińska-Cichocka, M., & Zganjar, E. (2012). New half-lives of r-process Zn and Ga isotopes measured with electromagnetic separation. *Physical Review Letters, 109* (11) https://doi.org/10.1103/PhysRevLett.109.112501

New Half-lives of r-process Zn and Ga Isotopes Measured with Electromagnetic Separation

M. Madurga *et al.*

Phys. Rev. Lett. **109**, 112501 — Published 13 September 2012

DOI: 10.1103/PhysRevLett.109.112501

New half-lives of r-process Zn and Ga isotopes measured with electromagnetic separation

M. Madurga[1], R. Surman[2], I.N. Borzov[3], R. Grzywacz[1,4], K. P. Rykaczewski[4], C.J. Gross[4], D. Miller[1], D.W. Stracener[4], J.C. Batchelder[5], N.T. Brewer[6], L. Cartegni[1], J.H. Hamilton[6], J.K. Hwang[6], S.H. Liu[5], S.V. Ilyushkin[7], C. Jost[1], M. Karny[5,8], A. Korgul[8,9], W. Królas[10], A. Kuźniak[1,8], C. Mazzocchi[8,9], A.J. Mendez II[4], K. Miernik[4,8], S.W. Padgett[1], S.V. Paulauskas[1], A.V. Ramayya[6], J.A.Winger[7], M. Wolińska-Cichocka[4,5], E.F. Zganjar[11]

[1]*Dept. of Physics and Astronomy, University of Tennessee, Knoxville, Tennessee 37996, USA*
[2]*Dept. of Physics, Union College, Schenectady, New York 12308, USA*
[3]*Joint Institute for Nuclear Research, 141980 Dubna, Russia*
[4]*Physics Division, Oak Ridge National Laboratory, Oak Ridge, Tennessee 37830, USA*
[5]*Oak Ridge Associated Universities, Oak Ridge, Tennessee 37831, USA*
[6]*Dept. of Physics and Astronomy, Vanderbilt University, Nashville, Tennessee 37235, USA*
[7]*Dept. of Physics and Astronomy, Mississippi State University, Mississippi 39762, USA*
[8]*Faculty of Physics, University of Warsaw, Warszawa PL 00-681, Poland*
[9]*Joint Institute for Heavy-Ion Reactions, Oak Ridge, Tennessee 37831, USA*
[10]*Institute of Nuclear Physics, Polish Academy of Sciences, Kraków, PL 31-342, Poland*
[11]*Dept. of Physics and Astronomy, Louisiana State University, Baton Rouge, Louisiana 70803, USA*

(Dated: September 6, 2012)

The β-decays of neutron-rich nuclei near the doubly magic ^{78}Ni were studied at the Holifield Radioactive Ion Beam Facility (HRIBF) using an electromagnetic isobar separator. The half-lives of ^{82}Zn (228$\pm$10 ms), ^{83}Zn (117$\pm$20 ms) and ^{85}Ga (93$\pm$7 ms) were determined for the first time. These half-lives were found to be very different from the predictions of the global model used in astrophysical simulations. A new calculation was developed using the Density Functional model, which properly reproduced the new experimental values. The robustness of the new model in the ^{78}Ni region allowed us to extrapolate data for more neutron-rich isotopes. The revised analysis of the rapid neutron capture process in low entropy environments with our new set of measured and calculated half-lives shows a significant redistribution of predicted isobaric abundances strengthening the yield of A>140 nuclei.

PACS numbers: 23.40.-s, 21.60.Jz, 26.30.Hj, 27.50.+e

The r-process nucleosynthesis, responsible for creating heavy elements [1], involves reactions and decays of unstable, neutron-rich isotopes of all elements between nickel and uranium. Its path and pace depends on the properties of neutron-rich isotopes far from nuclear stability. Many of these species have never been studied experimentally because of the challenges in producing and isolating them under laboratory conditions. Both experimental nuclear data and nuclear theory predictions are combined with astrophysical models to calculate abundance patterns of r-process elements [2–4], and the results are compared with measured solar abundances [5]. The nuclear shell structure [2] was found to have a strong imprint in the general abundance pattern, with major peaks aligned with shell closures. However, and not surprisingly given the models reliance on phenomenological simplifying assumptions, the detailed agreement is still rather poor. Although the astrophysical uncertainties remain a large part of the abundance calculations, improving the quality and reliability of the nuclear data can reduce the uncertainty of the r-process simulations.

Together with neutron capture rates and nuclear binding energies, β-decay half-lives are one of the nuclear properties that strongly influence the predicted isotopic distribution of nuclei produced in the astrophysical r-process [6, 7]. The nuclear half-life and mass are some of the few quantities accessible experimentally for very exotic isotopes. These observables can be determined with only a few atoms, which can be synthesized and separated by existing techniques [6, 8, 9]. This puts the masses and β-decay half-lives in a special position, as they often are the only known observables that can be used to benchmark the quality of theoretical models used to predict nuclear properties into regions beyond the reach of existing or planned facilities. Several global models were developed to calculate nuclear half-lives for all beta decaying nuclei, among them is the macroscopic-microscopic Finite Range Droplet Model with Quasi-particle Random Phase Approximation for excited states (FRDM+QRPA) [3, 10–12] and the so-called statistical gross theory [13] including its later semi-statistical version [14].

In this Letter we present the first measurement of the half-lives of neutron-rich isotopes directly on the predicted r-process boulevard [15], ^{85}Ga and ^{82,83}Zn. This measurement was made possible by the development [16] in the electromagnetic separation technique, which enabled measurement of nearly pure isotopic beams of the studied nuclei. We have found that the global models fail to reproduce the newly measured half lives of nuclei close to shell closures. The new data enabled us to verify the predictions of our microscopic β-decay model for spherical isotopes near the r-process path [17]. We investigated the influence of our new calculated decay half-lives on an r-process nuclear network calculation for low entropy environments, e.g., neutron star mergers. We observed that the updated values for isotopes near ^{78}Ni impact not only the final abundance pattern in their own mass region, but also the flow of material to the heaviest r-process nuclei (with increases greater than 200% for A>140).

A critical part of this difficult measurement was the production of very pure samples of zinc and gallium isotopes using the unique capabilities of direct electromagnetic isotope separation developed at the Holifield Radioactive Ion Beam Facility (HRIBF) at Oak Ridge National Laboratory [16] and demonstrated previously by the related study of ^{81}Zn [18]. A 50 MeV proton beam of 10 μA to 18 μA intensity was used to induce fission in a UC_x target (about 6 g/cm^2) located at the target ion source assembly mounted in the newly commissioned Injector for Radioactive Ion Species 2 at HRIBF [16]. Radioactive fission products were extracted as positive ions and selected using two consecutive mass-separation magnets with a nominal mass resolution $m/\Delta m$ approximately of 1000 and 10,000 respectively. Electromagnetic separation alone was able to produce beams of ^{82,83}Zn and ^{85}Ga with isotopic purity sufficient to enable a very clean lifetime measurement. One must note that, in each case, this separation technique was able to remove isobaric contaminants on the order of 10^6 more intense than the beam of interest. This achievement was reserved so far for the techniques relying on applications of the selective laser ionization techniques [9] or ion traps [19]. Electromagnetic separation does not depend on atomic properties as it is applicable to purifying more beams than those requiring lasers [9], or chemical selectivity [20].

In order to enable lifetime measurements, an electrostatic kicker periodically deflected the ion beam after the 2nd-stage separator. The separated ions were transmitted to the Low Energy Radioactive Ion Beam Spectroscopy Station (LeRIBSS) for decay measurements. The 200 keV ions were implanted into a tape in the Moving Tape Collector (MTC) in the middle of the β-γ counting setup. The MTC was operated in take-away mode with cycles of 4 seconds accumulation followed by 2 seconds decay measurement during which deflected the ion beam. After the decay part of the cycle, the MTC transported the collected samples approximately 50 cm away from the shielded measuring station within 400 ms. The γ and β radiations were measured using four high-purity Ge clover detectors and two plastic β scintillators surrounding the implantation point. The photo-peak efficiency for the closely packed geometry of the clover array was 34% at 81 keV and 6% at 1.33 MeV.

The half-lives were obtained by fitting the background-subtracted growth and decay patterns of the γ-transitions assigned to the β-γ or β-n-γ decay channels to the appropriate solution of the Bateman equations. In two cases we were able to determine half-lives with an accuracy better than 10%, and within 20% in the other case. This is a great advantage of the ISOL method over fragmentation facilities, where accuracies of 50% or worse are common due to

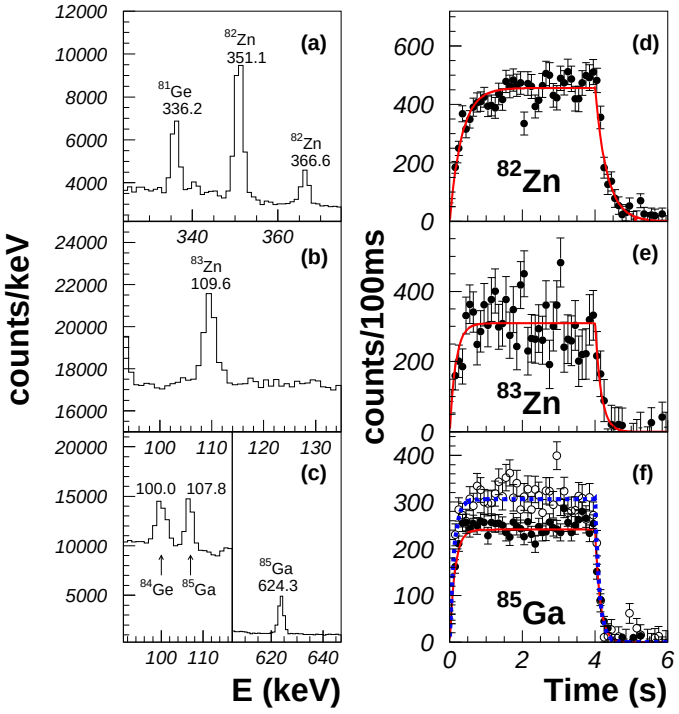

FIG. 1. (Color on-line) Left column: Portions of the β-gated γ-ray spectrum following the decay of ^{82,83}Zn and ^{85}Ga (a,b, and c) near the transitions used to determine the half-lives. The half-life of ^{82}Zn was calculated from the gate on the 351 keV peak. Transitions from the decay of the β-n granddaughter ^{81}Ge and daughter ^{84}Ge are marked. Right column: Growth and decay curves for ^{82,83}Zn and ^{85}Ga (d,e and f) obtained from the transitions shown in the left column. The data were fit to the Bateman equations, red lines, resulting in 228(10), 117(20) and 93(7) ms for ^{82,83}Zn and ^{85}Ga respectively. The ^{85}Ga half-life is the average of the fit of the 107 keV (○) and 624 keV (●) transitions.

the low production rates [6, 7, 21].

The left column of Fig. 1 (panels a, b and c) shows the region of the β-gated gamma spectra around the peaks used to determine the half-life marked by the assigned parent activity. The right column of Fig. 1 (panels d, e and f) displays the growth and decay patterns gated by the selected transitions with our best fit overlaid. Full results of the study of the ^{82,83}Zn and ^{85}Ga β-decays will be presented in separate publications, while here we describe the main decay properties. After the isobar separator was optimized for ^{82}Zn we identified two transitions at 351 and 451 keV, previously observed in the β-decay of ^{81}Zn into ^{81}Ga [18, 22]. This places these two transitions as following the βn decay of ^{82}Zn to the known excited states in ^{81}Ga. Due to the larger counting statistics in the 351 keV transition, the half-life analysis is based on the growth and decay pattern of 351 keV transition. From the χ^2 fit of the growth and decay curve (see Fig. 1d) we obtain a ^{82}Zn half-life of 228(10) ms with χ^2/n_{free}=1.07.

On the γ-ray spectrum for the decay of isobarically separated ^{83}Zn we observe a prominent transition at 109 keV (see Fig. 1b) previously unreported for the A=82 and A=83 isobars. By gating on this transition, subtracting background, and fitting the growth and decay curve, we obtain a half-life of 117(20) ms, with χ^2/n_{free}=1.04. This value is significantly shorter than the reported half-lives for the β-decay of the β-n daughters ^{82}Ga, 599(2) ms, and ^{82}Ge, 4.55(5) s [23], and isobars ^{83}Ga, 308(1) ms, and ^{83}Ge, 1.85(6) s [24]. This supports the placement of this transition in the β-decay of ^{83}Zn.

During the previous study of β-decay of ^{84}Ga and ^{85}Ga at HRIBF [25], the 624 keV γ-transition was assigned as the de-excitation of the first 2^+ state in ^{84}Ge. Our new data on ^{85}Ga decay confirm the 624 keV γ-line transition populated in the β-n branch (see Fig. 1c). Also, a previously unreported transition at 107 keV appears prominently with a half-life consistent with that of the 624 keV line (see Fig. 1c).

Since both transitions at 107 and 624 keV have similar statistics we used the growth and decay curves gated on each transition to obtain the ^{85}Ga half-life (see Fig. 1f). The resulting half-lives are 84(8) ms and 99(6) ms with χ^2/n_{free}=1.01 and 0.98 respectively. We adopt the weighted average of 93(7) ms as the ^{85}Ga half-life.

The new half-life values presented here for the Zn and Ga isotopic chains prompted us to reconsider the predictive power of global models in the neutron-rich region of nuclear chart. The large neutron proton imbalance gives rise

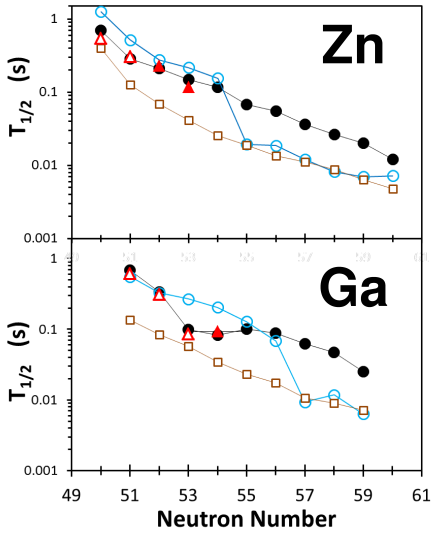

FIG. 2. (Color on-line) Half-lives of the Zn (top) and Ga (bottom) isotopic chains. Shown are: experimental values (△ [18, 23–27] and ▲, this work), FRDM+QRPA [12] (○), gross theory of beta-decay [28] (□), and a new energy density functional model (see text) (●). Our new calculation predicts a stabilization of the half-lives, compared to the global models.

to effects absent in nuclei closer to stability, which might play a prominent role in the β-decay. For nuclei with N>50, beta-decay models must include both Gamow-Teller (GT) and first-forbidden (FF) transitions since neutrons fill positive parity orbitals ($1g_{9/2}$, $2d_{5/2}$ and $3s_{1/2}$) and protons occupy negative parity ($1f_{5/2}$, $2p_{3/2}$ and $2p_{1/2}$). Moreover, the ordering of both proton and neutron shells is important, whether the valence neutrons are in the $2d_{5/2}$ or the $3s_{1/2}$ orbitals, as these FF transitions contribute a large share of the decay strength above the N=50 shell.

Testing the validity of the half-lives predicted by global models is important, as network calculations use them when no experimental information exists [12]. For the Zn and Ga isotopic chains, previous global model calculations overestimate the half-lives above the N=50 shell [18, 23–27] by a factor of about two, as shown in Fig. 2. Furthermore, above N=55 in the Zn chain and N=57 in the Ga chain, a rapid drop of the half-life values is predicted due to a sudden change of the calculations deformation framework. One notes that the half-life values calculated in the global model [12] above these thresholds become close to the gross theory predictions [28].

Our newly measured half-lives were compared to the predictions using the ground state properties as given by the recently developed DF3a [29] energy density functional tailored for neutron-rich nuclei around the N=50 and N=82 shell closures. The beta-strength functions for GT and FF decays were derived self-consistently within the DF3a +CQRPA model, using the method outlined in Ref. [30]. Our new calculation is an extension of the one that successfully reproduced the experimental neutron branching ratios obtained at HRIBF [31]. There, the model included the new values of masses in the region [32, 33], and the ground state configurations in odd-Z Ga isotopes up to A=83 were set to be $1f_{5/2}$ proton single-particle states by using the blocking approximation. This approach is consistent with the change in systematics of the spin and parity of the ground state of Cu isotopes [34, 35] (understood as driven by the proton-neutron interaction when filling the $\nu g_{9/2}$ shell [36]). We found that only the calculation that extended beyond A=83 the blocking of the ground state configuration to a $1f_{5/2}$ proton-single-particle state was able to reproduce the ^{85}Ga half-life value (see Fig. 2b). No other modifications or local adjustments were made to the model after the initial calibration in Ref. [31]. The half-lives calculated in both isotopic chains agree well with our new measurements, see Fig. 2a and b.

One must also note that the new experimental half-lives are shorter than the values obtained in the FRDM+QRPA model, and are essentially reproduced in our DF3a+CQRPA calculations. For Ga isotopes with N=54-59, where only extrapolations are available, our self-consistent model predicts stabilization of the half-lives beyond N=56. Importantly for r-process calculations (see below), the DF3a+CQRPA predicts significantly longer lifetimes than FRDM+QRPA for N>56.

Because the DF3a+CQRPA lifetimes strongly deviate from the predictions of the global model we investigated their potential impact on calculations of r-process nucleosynthesis. We performed dynamic nuclear network calculations [37] of the r-process with a sample parameterized trajectory from a compact object merger model [38]. Surprisingly, we found that not only can these half-lives influence the abundances in the 75<A<90 region, but they can impact

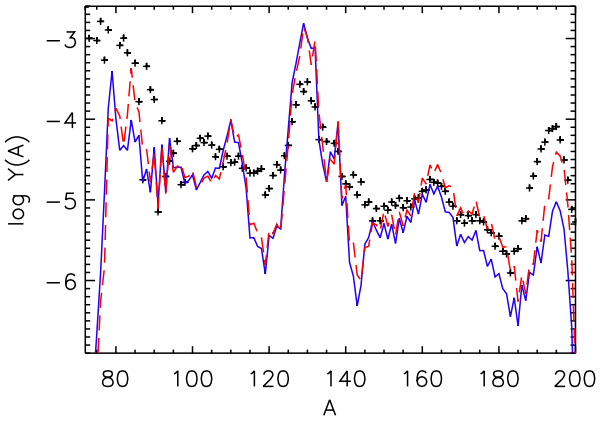

FIG. 3. (Color on-line) Calculated abundances for r-process nuclei, for a baseline simulation using FRDM [12] half-lives (solid blue line) and a simulation substituting half-lives for neutron rich isotopes ($27 \leq Z \leq 32$) obtained in the DF3a+CQRPA framework from this work (dashed red line). The black crosses show the solar residual (r-process) abundances from [5]. The thermodynamic conditions are from a low entropy ($s/k = 10$), fast outflow ($\beta = 0.2$), $\theta = 0$ trajectory from [37].

how the r-process proceeds for heavier nuclei, as shown in Fig. 3. In the baseline simulation with the global model half-lives used exclusively, the r-process abundance peaks around A=160 and A=195 are only partially populated. However, a significantly redistributed abundance pattern results, including a more vigorous production of nuclei above A>140, when the FRDM+QRPA half-lives are substituted with the values from currently available DF3a calculations for spherical nuclei in the vicinity of ^{78}Ni: $^{66-77}$Co, $^{72-86}$Ni, $^{74-89}$Cu, $^{82-90}$Ga, and $^{83-90}$Ge. This can be explained from the difference between our model and the global model half-lives for nuclei of mass above and below the threshold around N=56 (A=85). The longer DF3a+QRPA half-lives above A=85 cause more material to be trapped in the first peak, around A=80, compared to the baseline simulation. Since less material makes it past the first peak, fewer neutrons are depleted in this region, leaving more neutrons available for capture on A>90 nuclei and enhanced production of heavier species. A more detailed sensitivity study with a larger set of nuclei and thermodynamical conditions is in preparation [39].

In summary, the high beam intensity and purity achieved with the recently commissioned IRIS-2 ISOL platform at HRIBF has allowed us to determine the ^{85}Ga half-life and observe for the first time the β-decay of the ^{82,83}Zn. The half-life values presented here, measured with 10-20% uncertainty, were used to verify a new model using a recently developed energy density functional and requiring $\pi 1_f 5/2$ single particle ground state configuration. The differences between the half-lives of isotopes in the ^{78}Ni vicinity calculated in our locally calibrated model and in global models have a large effect on the predicted overall abundance pattern obtained from r-process calculations, with an increase of greater than 200% for some masses above A=140. The limitations of the global model to calculate properties of nuclei close to shell closures are apparent in the discrepancies with our experimental values This suggests that a new generation of models, with a more microscopic foundation, is required to provide reliable values for network calculations.

We thank the HRIBF operations staff for providing the excellent quality radioactive ion beams necessary for this work. Special thanks to W. Nazarewicz for the fruitful discussions. This research was sponsored in part by the National Nuclear Security Administration under the Stewardship Science Academic Alliances program through DOE Cooperative Agreement No. DE-FG52-08NA28552. This research was also sponsored by the Office of Nuclear Physics, U. S. Department of Energy under contracts DE-AC05-00OR22725 (ORNL), DE-FG02-96ER40983 (UTK) and DE-FG-05-88ER40407 (VU). The authors from University of Warsaw acknowledge the support by the Polish NCN under grant number 2011/01/B/ST2/02476. I.B. is partially supported within the IN2P3-RFBR agreement No.110291054.

[1] E. M. Burbidge, G. R. Burbidge, W. A. Fowler, and F. Hoyle, Rev. Mod. Phys. **29**, 547 (1957).
[2] K.-L. Kratz *et al.*, Astrophys. J. **403**, 216 (1993).
[3] T. Rauscher *et al.*, Phys. Rev. C **57**, 2031(1998).
[4] K. Langanke and G. Martinez-Pinedo, Rev. Mod. Phys. **75**, 819 (2003).
[5] C. Sneden, J.J. Cowan, and R. Gallino, Annu. Rev. Astro. Astrophys. **46**, 241 (2008).
[6] P. Hosmer *et al.*, Phys. Rev. Lett. **94**, 112501 (2005).
[7] S. Nishimura *et al.*, Phys. Rev. Lett. **106**, 052502 (2011).
[8] M. Bernas *et al.*, A **616**, 352 (1997).
[9] J. Shergur *et al.*, Physical Review C **65**, 034313 (2002).
[10] P. Möller, J.R. Nix, W.D Myers, and W.J. Swiatecki, Atom. Data Nucl. Data **59**, 185 (1995).
[11] P. Möller, J.R. Nix, and K.-L. Kratz, Atom .Data Nucl. Data **66**, 131 (1997).
[12] P. Möller, B. Pfeiffer, and K.-L. Kratz, Phys. Rev. C **67**, 055802 (2003).
[13] K. Takahashi, Prog. Theor. Phys. **45**, 1466 (1971).
[14] H. Nakata, T.Tachibana, and M.Yamada, Nucl. Phys. A **625**, 521 (1997).
[15] K.-L. Kratz, AIP Conference Proceedings, Vol. 819, 409 (2006).
[16] J.R. Beene *et al.*, J. Phys. G: Nucl. Part. Phys. **38**, 024002 (2011).
[17] I.N.Borzov, in *Proceedings of the NATO Advanced Research Workshop on Nuclear Many-Body Problem, Brijuni, Croatia, 2001*, edited by W. Nazarewicz and D. Vretenar (Kluwer, Dordrecht 2002), p. 323.
[18] S. Padgett *et al.*, Phys. Rev. C **82**, 064314 (2010).
[19] S. Rinta-Antila *et al.*, Eur. Phys. J. **A31**, 1 (2007).
[20] H.L. Ravn, Nucl. Instrum. & Methods **B**70, 107 (1992).
[21] P. Hosmer *et al.*, Phys. Rev. C **82**, 025806 (2010).
[22] D. Verney *et al.* Phys. Rev. C **76**, 054312 (2007).
[23] J.K. Tuli, Nucl. Data Sheets, **98**, 209 (2003).
[24] S.-C. Wu, Nucl. Data Sheets, **92**, 893 (2001).
[25] J.A. Winger *et al.*, Phys. Rev. C **81**, 044303 (2010).
[26] B. Singh, Nucl. Data Sheets **105**, 223 (2005).
[27] D. Abriola *et al.*, Nucl. Data Sheets **110**, 2815 (2009).
[28] H. Nakata, T. Tachibana, M. Yamada, Nucl. Phys. A **625**, 521 (1997).
[29] S. V. Tolokonnikov and E. E. Saperstein, Phys. Atom. Nucl. **73**, 1684 (2010).
[30] I.N. Borzov, Phys. Rev. C **67**, 025802 (2003).
[31] J. Winger *et al.*, Phys. Rev. Lett. **102**, 142502 (2009).
[32] J. Hakala *et al.*, Phys. Rev. Lett. **101**, 052502 (2008).
[33] S. Baruah *et al.*, Phys. Rev. lett. **101**, 262501 (2008).
[34] S.V. Ilyushkin *et al.*, Phys. Rev. C **80**, 054304 (2009).
[35] K. Flanagan *et al.*, Phys. Rev. Lett. **103**, 142501 (2009).
[36] T. Otsuka, T. Suzuki, R. Fujimoto, H. Grawe, and Y. Akaishi, Phys. Rev. Lett. **95**, 232502 (2005).
[37] R. Surman and J. Engel, Phys. Rev. C **64**, 035801 (2001).
[38] R. Surman, G.C. McLaughlin, M. Ruffert, H.-Th. Janka, and W.R. Hix, Astrophys. J., **679**, L117 (2008)
[39] R. Surman *et al.*, in preparation.